Proceedings of the 12th International Conference on
Aluminium Alloys, September 5-9, 2010, Yokohama, Japan
©2010 The Japan Institute of Light Metals
pp. 469-474

The Effect of Bimodal Precipitate Distributions on the Strength-Elongation Combinations in Al-Cu Alloys

Yu Chen[1], Matthew Weyland[2] and Christopher R. Hutchinson[1]

[1]ARC Centre of Excellence for Design in Light Metals, Department of Materials Engineering, Monash University, 3800 VIC, Australia

[2]Monash Centre for Electron Microscopy (MCEM), Monash University, 3800 VIC, Australia

The yield strength and uniform elongation combinations exhibited by a model Al-4Cu-0.05Sn (wt. %) alloy containing a bimodal size distribution of precipitates has been investigated. The simultaneous improvement in properties previously reported from such precipitate distributions is confirmed through mechanical tests. In particular, the bimodal sized precipitate containing alloy shows enhanced strain-hardening at large strains and this is the origin of the enhanced elongation. Transmission electron microscopy (TEM) and scanning transmission electron microscopy (STEM) were used to characterize the microstructures of the undeformed and deformed alloys. It is shown that the magnitude of the enhanced strain-hardening is consistent with that expected from the strain-induced dissolution of GP zones and concurrent repartitioning of Cu into solid solution.

Keywords: *yield strength, uniform elongation, strain-hardening, dissolution, interrupted ageing*

1. Introduction

The yield strength (σ_y) and uniform elongation (ε_u) are both important properties of engineering alloys. In precipitation hardenable alloys, these properties are directly related to the interaction between the precipitates and mobile dislocations, and typically show an inverse correlation. It has recently been shown that, through careful control of the precipitate structures, it is possible to obtain simultaneous improvements in both σ_y and ε_u [1,2]. This simultaneous improvement is of considerable technological significance and may open up possibilities for the development of new alloys if the physical origin of the improvements can be identified.

The quantitative relationship linking microstructure and yield strength (σ_y) is relatively well developed for precipitation hardened materials, especially those containing shear-resistant precipitates, e.g. [3-5]. The link between microstructure and elongation is less clear. For materials that fail in a ductile manner, Considère's criterion (i.e. necking is reached when the flow stress, σ_f, is equal to the strain-hardening rate: $\sigma_f = d\sigma_f/d\varepsilon$) is often used to calculate the uniform elongation (ε_u). Using this criterion, ε_u depends on the strain-hardening behaviour $d\sigma_f/d\varepsilon$, which needs to be explicitly described as a function of the precipitate state. For pure face-centered cubic (FCC) metals, the phenomenological strain-hardening model developed by Kocks and Mecking (KM) [6] is often used. Attempts have been made by various authors to incorporate the effect of precipitates into the KM model [7-9]. Most recently, da Costa Teixeira *et al*. [9] developed a reasonably detailed description of the strain-hardening behaviour of an Al-Cu alloy containing exclusively shear resistant θ′ that considered both isotropic and kinematic hardening. The model showed good agreement with experimental results. An opportunity now exists to extend this work to consider the strain-hardening of alloys containing both shear-resistant and shearable precipitates in an effort to identify the physical origin of the enhanced properties exhibited by bimodal precipitate containing Al alloys. This is the objective of this study.

A model alloy of composition Al-4Cu-0.05Sn (wt.%) was chosen to investigate the effects of bimodal precipitate distributions because, through suitable heat treatment, a uniform and controllable distribution of shear-resistant θ′ (Al_2Cu) precipitates and shearable GP zones can be formed and models for the strengthening and strain-hardening behaviour in alloys containing θ′ are currently available [5,9].

2. Experimental Procedure

An alloy of composition Al-4Cu-0.05Sn (wt. %) was prepared from high purity elements by sand casting. The ingots were homogenized at 550°C for 72h, and then hot rolled into sheets of 3mm thickness for tensile sample preparation. The samples were solution treated at 520°C for 1h, rapidly quenched in water, and then aged at 200°C (isothermal ageing) or 65°C (interrupted ageing). The isothermal ageing was performed for a range of times up to 30 days in oil to form shear-resistant θ′ precipitates. The interrupted ageing was performed at 200°C for 10 minutes, followed by direct transfer to an oil bath at 65°C for a period of times up to 30 days.

The precipitate microstructures were initially characterized using a Philips CM-20 transmission electron microscope (TEM), operating at 200 kV. High-resolution imaging was carried out in high angle annular dark field (HAADF) scanning TEM (STEM) mode on an aberration corrected FEI Titan^3 80-300 TEM, operating at 300 kV. Foils were prepared from the gauge sections for plastically deformed or the grip regions for undeformed specimen of tensile samples. Discs were punched with 3 mm diameters and gently ground to approximately 150 μm in thickness. These discs were then electro-polished using a conventional twin-jet polishing technique in a solution of 33% nitric acid and 67% methanol at -25°C using a voltage of 13 V.

Tensile tests were carried out using an Instron tensile testing machine with a strain rate of ~ $10^{-3}s^{-1}$ at room temperature. For each condition at least three tensile tests were performed. Tension-compression (Bauschinger) tests were preformed at the same strain rate to quantify the kinematic hardening contribution (not reported here) of the alloy after interrupted ageing.

3. Results

3.1 Ageing hardening response

Tensile tests were conducted in the as-quenched state (AQ), after isothermal ageing at 200°C for a range of times up to 30 days, and after interrupted ageing at 65°C for 7 days, 15 days and 30 days. The yield strength σ_y (0.2% proof stress) and uniform elongation ε_u (defined as the plastic strain for which the applied load is at the maximum) combinations exhibited are summarised in Fig. 1.

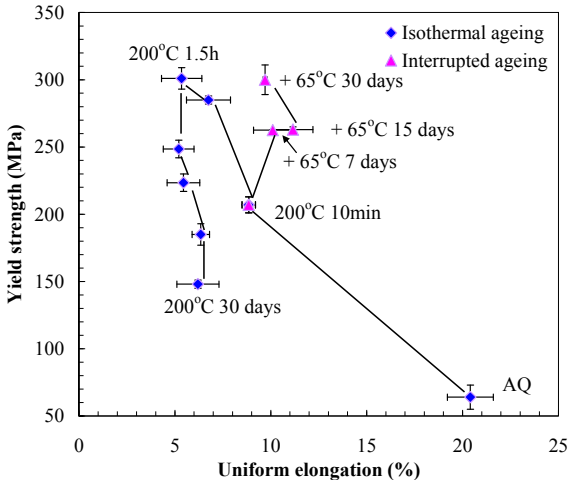

Fig. 1. Yield strength and uniform elongation combinations of the alloy after the isothermal ageing (blue diamonds) and the interrupted ageing (pink triangles).

The diamonds in Fig. 1 correspond to samples isothermal aged at 200°C. As is typically observed, an inverse correlation exists between σ_y and ε_u. The σ_y increases from an as-quenched (AQ) value of ~60MPa to ~200MPa after 10min aging and reaches a maximum of 300MPa after 1.5h. The ε_u correspondingly decreases from ~20% in the AQ state to ~5% after 1.5h aging at 200ºC.

The σ_y and ε_u of the samples after interrupted ageing are represented by the triangles in Fig. 1. After aging for 7 or 15 days at 65ºC, the σ_y increases from the value for the 10min 200ºC sample by ~50MPa and ε_u increases by 1-2%. After 30 days aging at 65ºC, an increase in σ_y of ~100MPa is observed without a decrease in ε_u. The simultaneous improvement of σ_y and ε_u reveals that the inverse

correlation usually observed between these properties can be broken and confirms that it is possible to simultaneously increase σ_y and ε_u using bimodally sized precipitate distributions [2].

It is worth highlighting the σ_y and ε_u combinations exhibited by the peak aged (1.5h) sample and the sample aged for 30 days at 65ºC (Fig. 1). These samples have the same σ_y (300MPa) but the 30 day sample has an ε_u of 10% compared with 5% for the peak aged (PA) state.

3.2 Precipitation microstructure

The microstructures of the isothermally UA (10 min) and PA (1.5h) samples were characterized using conventional TEM. Bright field micrographs are shown in Fig. 2a and b. The θ′ precipitates are the only precipitates observed and they form with a relatively uniform and homogeneous distribution. The microstructure of the alloy after interrupted ageing at 65°C for 30 days was characterized using TEM and STEM. A bright field TEM image is shown in Fig. 2c and a high angle annular dark field (HAADF) image is shown in Fig. 2d. The GP zones that form during the aging at 65ºC are observed between the θ′ precipitates in Fig. 2c. Quantitative measurements of the lengths of θ′ precipitates were made before and after aging at 65ºC and no change was observed. This is consistent with expectations based on diffusional growth theory. The HAADF image of the GP zones (Fig. 2d) shows that they consist of single atomic layers of Cu atoms.

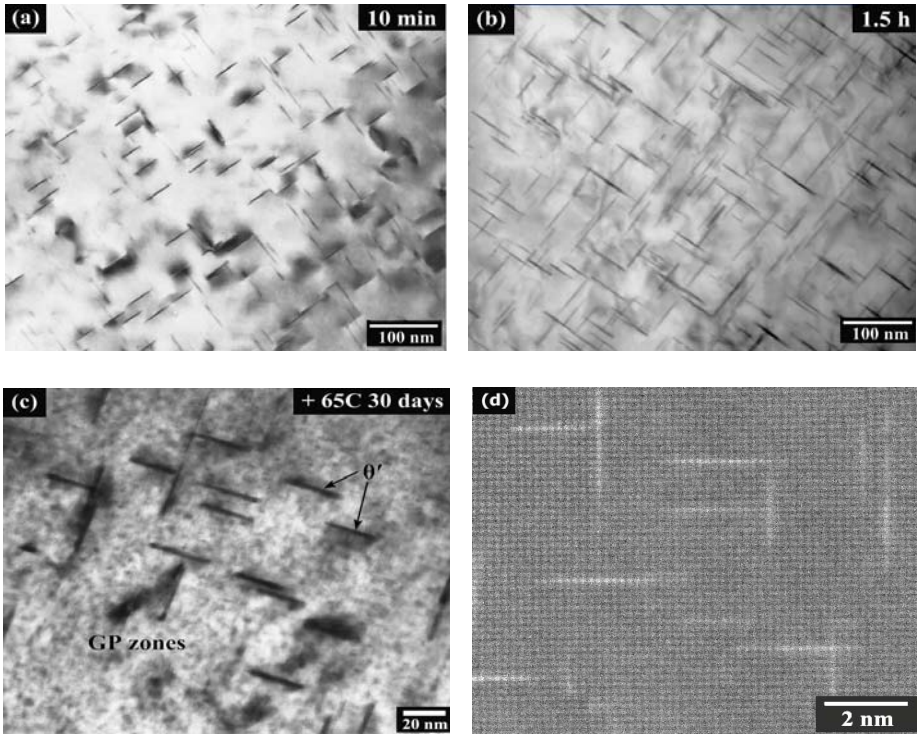

Fig. 2 TEM micrographs of the precipitate structure after (a) isothermal ageing at 200°C for 10 min (UA), (b) isothermal ageing at 200°C for 1.5h (PA), (c) interrupted ageing at 65°C for 30 days and (d) HAADF image of the sample in (c). The electron beam is close to $[001]_\alpha$.

To summarize, the TEM observations illustrate the formation of a fine distribution of GP zones during aging at 65ºC with no significant change in the θ′ precipitate distribution.

3.3 Strain-hardening behaviour

The strain-hardening behaviour of samples aged isothermally at 200ºC for 10min, and subsequently aged at 65ºC, as a function of strain, is shown in Fig. 3. The true stress-true strain curves are drawn ending at the ultimate tensile strength (UTS). It can be seen that Considère′s criterion works very well in each case since the intersection of σ_f and θ ($d\sigma_f/d\varepsilon$) is within 0.5% of the strain at which the UTS is reached.

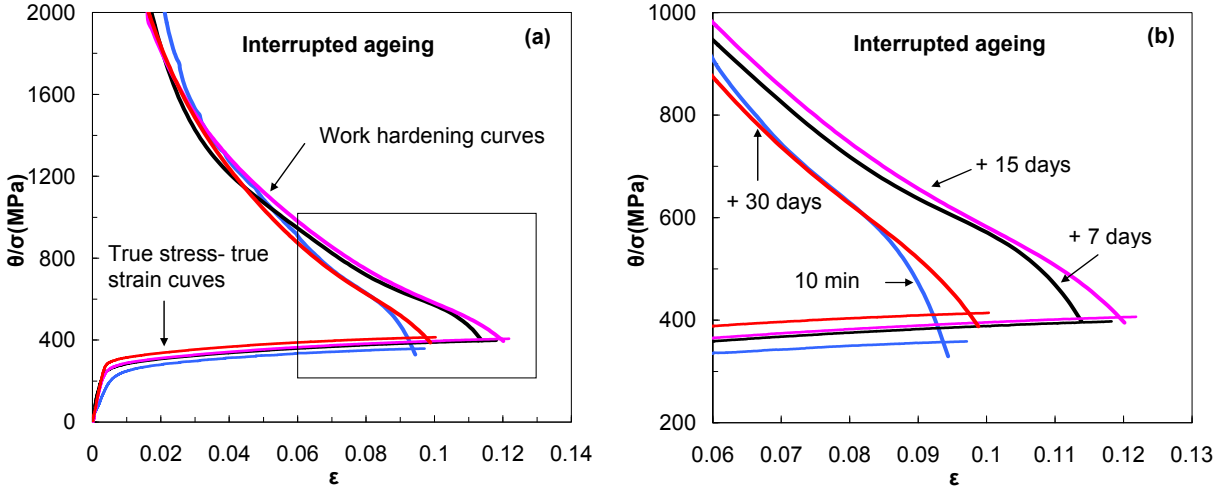

Fig. 3 (a) The comparison of the strain-hardening behaviour θ ($d\sigma_f/d\varepsilon$) of the alloys aged for: 200°C 10min, 200°C 10min + 65°C 7days, 15 days and 30days and (b) magnification of the boxed area in (a).

It is clear that the strain-hardening behaviour for each of the 4 states is essentially identical at low strains (2-5%). However, a clear difference is observed at larger strains. An enhanced strain-hardening is observed in the alloys aged at 65ºC (especially after ageing for 7 and 15 days), at the larger strains approaching necking. At a strain of 10%, the enhanced hardening is of the order of 200MPa in Fig. 3b. These results are consistent with the enhanced ε_u observed after interrupted ageing and with previous reports of the hardening exhibited in similar alloys [10].

4. Discussion and Conclusion

The origin of the enhanced σ_y after interrupted ageing is relatively clear. The GP zones are additional obstacles to dislocation motion and give rise to an increased yield stress. The more surprising result is the enhanced strain-hardening observed in the alloys containing GP zones and the resulting increase in ε_u. As shown in Fig. 2d, GP zones are single atomic planes of Cu. They are sheared by gliding dislocations. As a result, they are not thought to contribute to the dislocation storage that is usually the most important factor in enhancing the strain-hardening at large strains.

The key question is then: what is the origin of the enhanced strain-hardening?

There are two contributions to the strain-hardening of alloys containing shear resistant precipitates such as θ′: kinematic hardening and isotropic hardening.

The kinematic hardening is due to a long-range internal stress that opposes the direction of plastic straining and arises from plastic incompatibilities within the material (such as between θ′ and the matrix). It would not be surprising if, after interrupted ageing at 65°C, the high number density of GP zones promoted slip localization, and the accommodation of this localization at the grain boundaries gave rise to an intergranular contribution to the kinematic hardening. Bauschinger tests (not reported here) have been performed on samples before and after aging at 65ºC (i.e. with and without GP zones) and no additional contribution to the kinematic hardening is observed. In addition, optical microscopy of the polished surfaces of deformed samples shows that rather than promote strain localization, the GP zones actually impede the localization.

The isotropic contribution to the strain-hardening is independent of the direction of straining and is strongly influenced by the presence of shear-resistant precipitates. However, GP zones are shearable and are not thought to influence the isotropic hardening (except perhaps in a negative sense by removing solute from solution).

A possible explanation for the beneficial effect of the GP zones on the strain hardening at large strains was recently proposed [10] by invoking the idea of strain-induced dissolution of GP zones during deformation. These authors suggested that during deformation, the GP zones may partially

dissolve and the dynamic repartitioning of Cu from the GP zones to the matrix may lead to an enhanced isotropic contribution to the strain hardening through a strain dependant solute effect on the strength of dislocation junctions. It has since been shown using Nuclear Magnetic Resonance (NMR) measurements, that strain-induced dissolution of GP zones does occur in these alloys [11] and that the concentration of Cu in solid solution does have a strong effect on the strength of dislocation junctions in Al-Cu solid solutions [12].

In the present study, HAADF imaging was used to characterize the microstructure of the sample aged at 65°C for 30 days, before and after 10% tensile deformation. Quantitative measurements of the size and number density of GP zones before and after deformation illustrate that ~50% of the GP zones dissolve during the deformation. This is consistent with previous reports [11].

To test the quantitative feasibility of a shear-induced GP zone dissolution process being responsible for the enhanced strain-hardening, calculations based on the recent strain-hardening model of da Costa Texieira *et al*. [9] have been performed. da Costa Teixeira *et al.* presented a dislocation-based model to describe the yield and flow stress behaviour of an Al-Cu alloy containing only shear-resistant θ′ precipitates. Five contributions to the flow stress were considered (Eq. 1):

$$\sigma_f = \sigma_0 + \sigma_{ss} + (\sigma_{\theta'}^2 + \sigma_d^2)^{1/2} + <\sigma> \quad (1)$$

σ_0 is the intrinsic lattice stress, σ_{ss} is the solid solution hardening contribution, $\sigma_{\theta'}$ is the strengthening increment from θ′ precipitates, σ_d is the strength due to the dislocation forest and $<\sigma>$ is the internal stress. This model was capable of describing the combinations of strength and elongation exhibited by these alloys as a function of precipitate state. This model has been applied to the samples treated for 10min at 200°C (i.e. containing only θ′) in this study. Using the same parameters and approach outlined in [9], the calculated flow stress and strain-hardening behaviour is shown in Fig. 4. The experimental behaviour is well reproduced.

To incorporate the effect of GP zones formed during aging at 65°C, the approach has been modified to include a contribution to the flow stress from GP zones (Eq. 2):

$$\sigma_f = \sigma_0 + \sigma_{ss} + \sigma_{GP} + (\sigma_{\theta'}^2 + \sigma_d^2)^{1/2} + <\sigma> \quad (2)$$

σ_{GP} is the contribution to the strength from the GP zones and is assumed to sum linearly with the other contributions to the flow stress.

The net increase in yield strength resulting from the formation of GP zones is ~100MPa for the samples aged for 30 days at 65°C (Fig. 1). The NMR results previously reported [11] indicate, under these conditions, approximately 60% of the Cu is stored in GP zones. As a result the amount of Cu in solid solution and the contribution to solid solution strengthening can be calculated [5]. Consequently, the total GP zone strengthening contribution can be estimated so that the net increase in yield strength of ~100MPa (Fig. 1) is achieved. This is the assumed starting state.

To test the feasibility of strain induced GP zone dissolution as an origin of the enhanced strain-hardening, the following assumptions are made for the purpose of calculation: i) based on the previously reported NMR study, it is assumed that during straining to 10%, approximately 15-20% of the GP zones dissolve and that this dissolution occurs linearly with strain [11], ii) the subsequent decrease in the contribution of the GP zones to the flow stress varies linearly with the total amount (volume fraction) of GP zones, and iii) the additional Cu that is repartitioned into the matrix phase affects the dislocation-dislocation junction strength (α in Taylor's Eq: $\sigma_d = \alpha MGb\sqrt{\rho}$, where M is Taylor's factor, G is the shear modulus, b is Burgers vector and ρ is the dislocation density) in the manner quantitatively described in [12].

These assumptions are sufficient for a calculation of the expected net effect of the strain-induced dissolution of GP zones on the strain hardening behaviour to be made. The result is shown in Fig.4. It is clear that the dissolution of GP zones can lead to an enhanced strain-hardening at large strains and the magnitude of the increase (~200MPa at a strain of 0.1) over and above the sample containing only θ` is approximately consistent with the experimental observations (Fig. 3b).

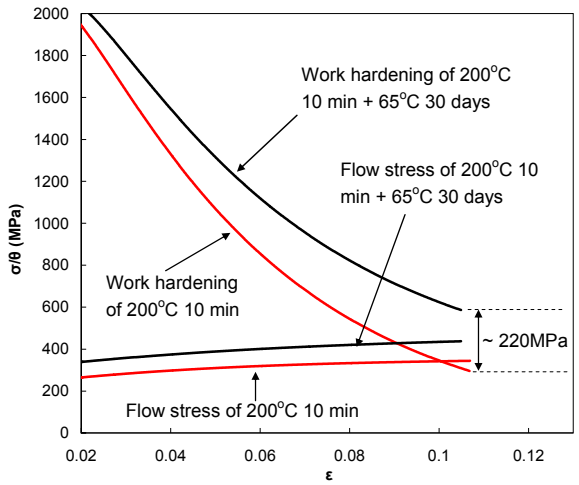

Fig. 4. Calculation of the true stress and strain-hardening vs. true strain behaviour of the alloys after ageing at 200°C for 10 min and after interrupted ageing at 65°C for 30 days.

The calculations shown in Fig. 4 should not be viewed as proof that the enhanced strain-hardening at large strains is due to the strain-induced dissolution of GP zones. Rather, it illustrates that using reasonable values of the input parameters, the magnitude of the expected effect on strain-hardening is consistent with that observed experimentally and the strain-induced dissolution behaviour is a possible explanation that deserves the attention of further research.

Acknowledgements: This work is supported by the Australian Research Council (ARC) through the ARC Centre of Excellence for Design in Light Metals. CRH gratefully acknowledges the support of the ARC through the award of a Future Fellowship. YC also gratefully acknowledges the support of China Scholarship Council (CSC). MW and MCEM acknowledge the support of ARC Linkage Infrastructure, Equipment and Facilities (LIEF) scheme and Nanotechnology Victoria Ltd.

References

[1] R. N. Lumley, I. J. Polmear, A. J. Morton, International Patent Application PCT/AU00/01601, (2000).
[2] R. N. Lumley, I. J. Polmear, A. J. Morton, Mater. Sci. and Tech. 21 (2005) 1025-1032.
[3] V. Gerold: *Dislocations in Solids*, Ed. by F. R. N. Nabarro, (North-Holland, 1979) pp. 219-260.
[4] A. J. Ardell, Metall. Trans. A 16 (1985) 2131-2165.
[5] J. D. Teixeira, D. G. Cram, L. Bourgeois, T. J. Bastow, A. J. Hill, C. R. Hutchinson, Acta Mater. 56 (2008) 6109-6122.
[6] U. F. Kocks, H. Mecking, Prog. Mater. Sci. 48 (2003) 171-273.
[7] Y. Estrin: *Unified Constitutive Laws of Plastic Deformation*, Ed. By A. Krausz, K. Krausz, (Academic Press, San Diego, 1996) pp. 69-106.
[8] A. Simar, Y. Brechet, B. Meester, A. Denquin, T. Pardoen, Acta Mater. 55 (2007) 6133-6143.
[9] J. D. Teixeira, L. Bourgeois, C. W. Sinclair, C. R. Hutchinson, Acta Mater. 57 (2009) 6075-6089.
[10] C. R. Hutchinson, L. Bourgeois and J.D. Teixeira, in Proceedings of the 11th International Conference on Aluminium Alloys, p. 1647-1652, (Aachen, Germany, 2008).
[11] C. R. Hutchinson, P. T. Loo, T. J. Bastow, A. J. Hill, J. D. Teixeira, Acta Mater. 57 (2009) 5645-5653.
[12] J. D. Teixeira, Y. Brechet, Y. Estrin, C. R. Hutchinson, elsewhere in Proceedings of the 12th International Conference on Aluminium Alloys, (Yokohama, Japan, 2010).